Discovery of a periodical apoastron GeV peak in LS I +61°303

F. Jaron, M. Massi (fjaron, mmassi@mpifr-bonn.mpg.de)
Max Planck Institute for Radioastronomy, Bonn, Germany

The stellar system LS I +61°303

consists of a Be star and a compact object in an eccentric orbit[1,2] with orbital period $P_1 \approx 26.5$ d.[3] Radio outbursts are observed at orbital phases Φ = 0.5-0.9, i.e., around apoastron, further modulated in amplitude and orbital phase by a long-term period $P_{long} \approx 1667$ d.[3] The GeV gamma-ray lightcurve has so far been reported to peak at orbital phases around periastron[4,5]

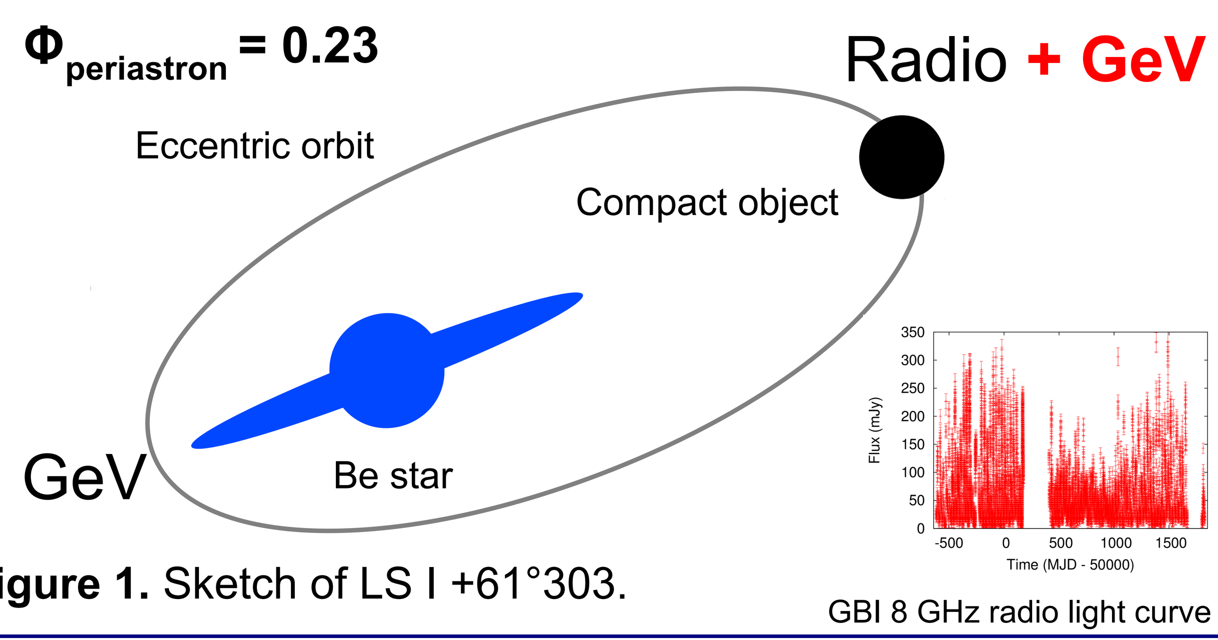

Figure 1. Sketch of LS I +61°303.

GBI 8 GHz radio light curve

Previous results[4,5]: The orbital period in GeV gamma-rays

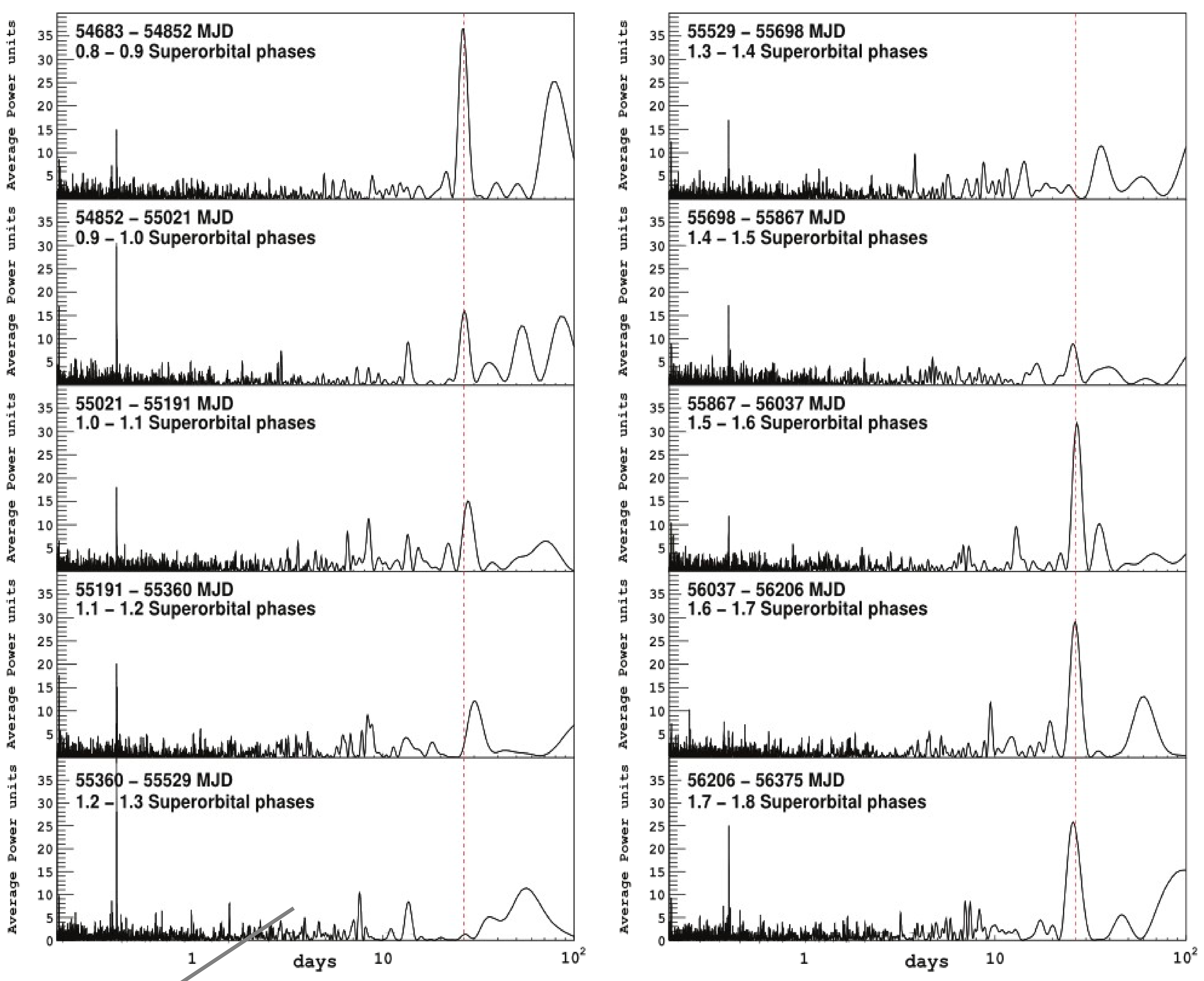

Lomb-Scargle timing analysis of *Fermi* LAT gamma-ray data from LS I +61°303 shows that the orbital period is present in the power spectrum, but not with equal power all of the time. **There are times of strong periodicity, and there are times when the orbital period is completely absent from the power spectrum[4].** This is shown in Fig. 2, where one cycle of the long-term period[3] $P_{long} \approx 1667$ d has been divided into ten bins[4]. The disappearance of the orbital period from the power spectrum is consistent with the previous findings[5].

Figure 2. Lomb-Scargle periodograms of *Fermi* LAT data from LS I +61°303 (Fig. 4 in ref. 4).

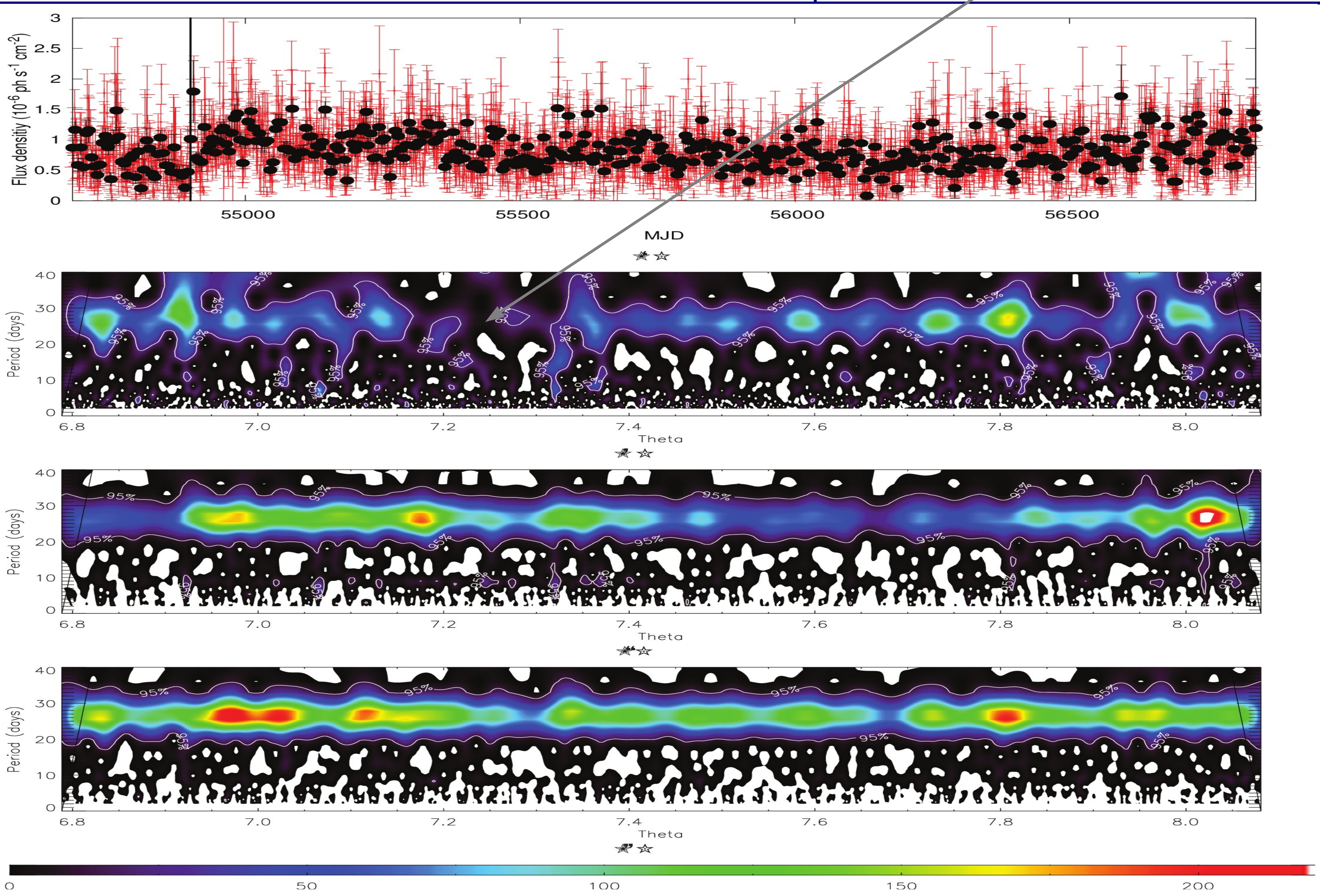

Figure 3. Light curve and wavelet plots of *Fermi* LAT data from LS I +61°303.

Wavelet analysis of *Fermi* LAT data from LS I +61°303

The gamma-ray data used in this analysis span the time period MJD 54683 (August 05, 2008) to MJD 56838 (June 30, 2014). The plot in the top panel of Fig. 3 shows the wavelet plot of the entire *Fermi* LAT data from LS I +61°303 of this period. The absence of orbital periodicity around Θ ≈ 7.2 (long-term phase[3], $P_{long} \approx 1667$ d) is consistent with the previous finding shown in Fig. 2. When wavelet analysis is performed only on data from the orbital phase intervals Φ = 0.0 - 0.5 (middle) and Φ = 0.5 - 1.0 (bottom), it is revealed that **there is always a periodic signal at Φ = 0.0 - 0.5 (periastron). Moreover, there is a periodic signal at Φ = 0.5 - 1.0 (apoastron)**. The latter becomes particularly strong during the time when the orbital period is absent from the power spectra.[6]

The newly discovered periodic apoastron peak in the GeV gamma-ray emission of LS I +61°303

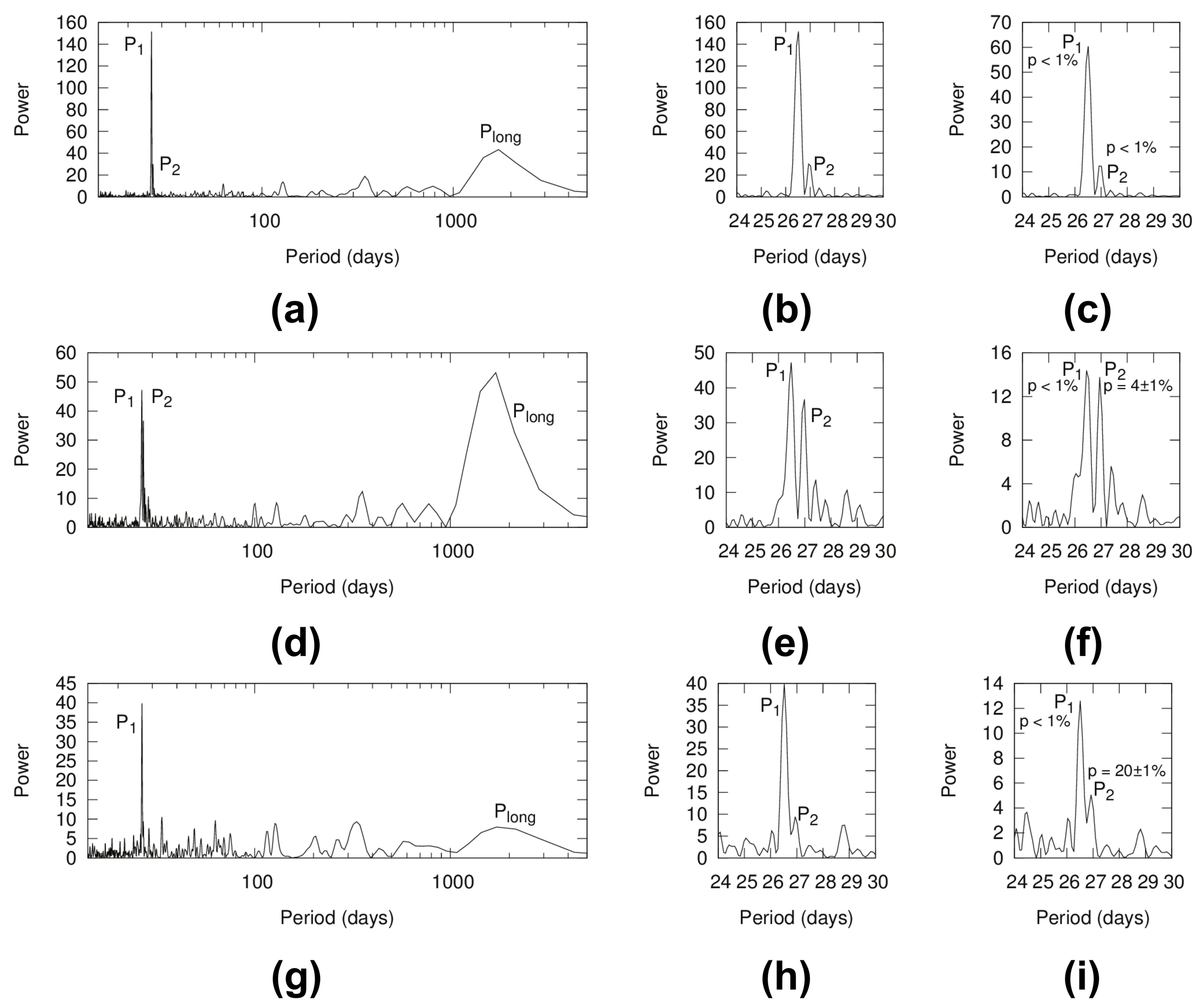

Figure 4. Lomb-Scargle periodogram of the *Fermi*-LAT data (with a time bin of one day). Figure 3 in Ref. 6. **(a)** Data in the orbital phase Φ = 0.0 - 1.0. **(b)** Zoom of Fig. 4 a. **(c)** Same as 4 b for data with a time bin of 5 d. **(d)** Data in the orbital phase Φ = 0.5 - 1.0. The periods P_2 and P_{long} here present are typical periodicities in radio data[7]. **(e)** Zoom of Fig. 4 d. **(f)** Same as 4 e for data with a time bin of 5 d. **(g)** Data in the orbital phase Φ = 0.0 - 0.5. **(h)** Zoom of Fig. 4 g. **(i)** Same as 4 h for data with a time bin of 5 d.

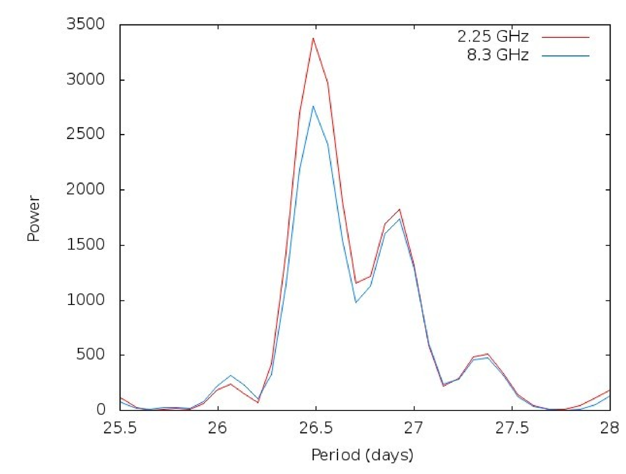

Figure 5. Timing analysis of 6.7 years of GBI radio data at 2.3 and 8.25 GHz results in two periods
$P_1 = 26.49 \pm 0.7$ d,
$P_2 = 26.92 \pm 0.7$ d,
the long-term period
$P_{long} = 1667 \pm 8$ days
is consistent with the period
$P_{beat} = 1/(\nu_1 - \nu_2) = 1667 \pm 393$ d
resulting from the beating between the two close periodicities P_1 and P_2.[7]

Apoastron: Both radio and GeV data feature the two periodicities P_1 and P_2.

Periastron: GeV data are only modulated by P_1.

The apoastron GeV peak in folded *Fermi* LAT data and its orbital shift

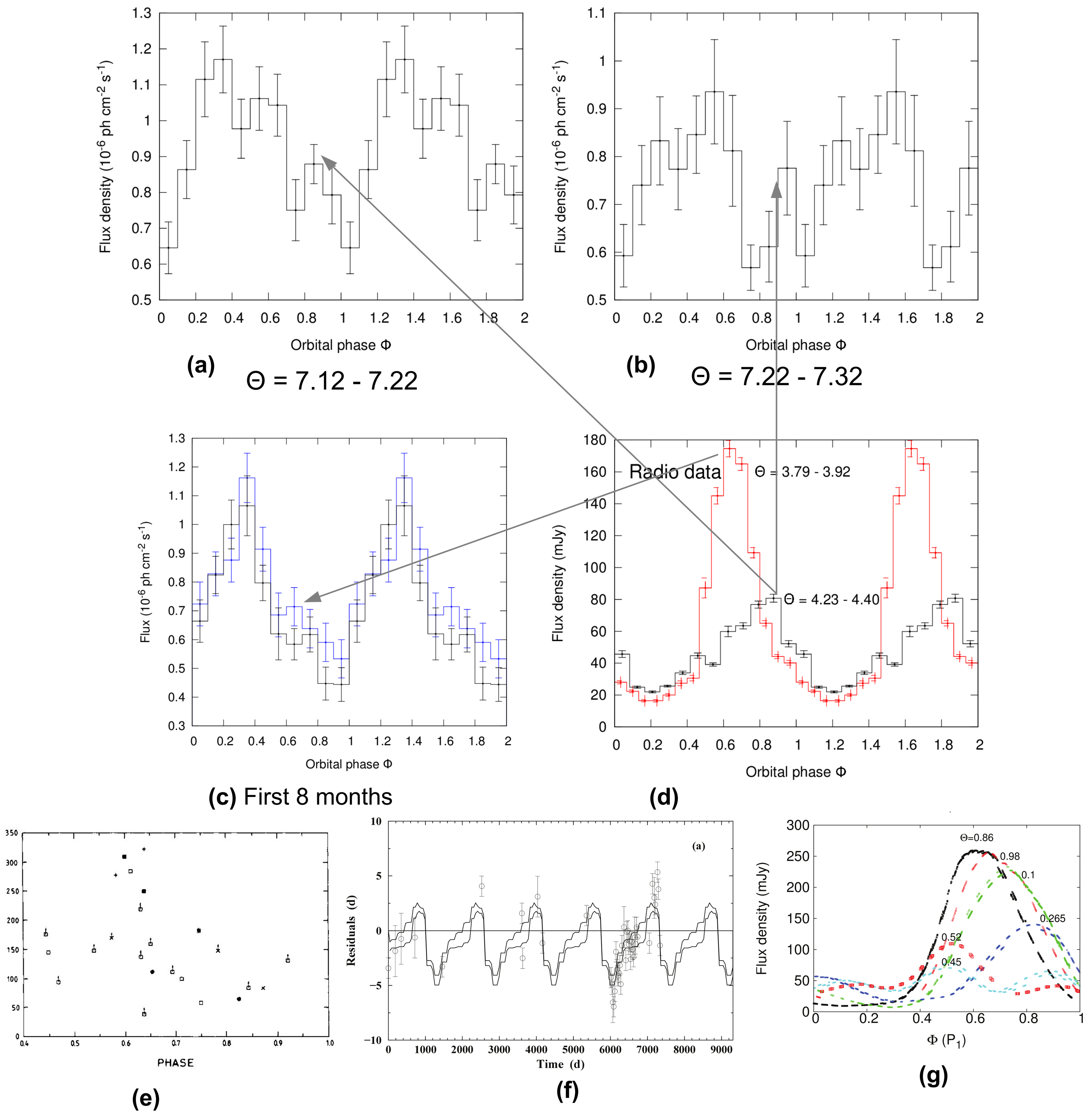

Figure 6. (a)-(c) Folded *Fermi* LAT gamma-ray data (100 MeV - 300 GeV). **(d)** Folded GBI 8 GHz radio data. **(e)** Orbital phase shift of the radio outburst[8]. **(f)** Timing residuals of the radio outbursts[9]. **(g)** Predicted orbital phase occurence of the radio outbursts[10].

Conclusions: During the intervals where the orbital periodicity is absent from the power spectra, wavelet and the folded light curves show two periodic signals, one at periastron and a second at apoastron (Fig 6 a-b). The presence of the second periodic outburst disturbs the timing analysis and prevents it from finding the orbital periodicity. Comparison with the folded radio data (Fig. 6 d) suggests that the apoastron GeV peak follows the same trend as the radio outbursts.[6]

References
1 Casares, J., Ribas, I., Paredes, J. M., Martí, J., & Allende Prieto, C. 2005, MNRAS, 360, 1105
2 Grundstrom, E. D., Caballero-Nieves, S. M., Gies, D. R., et al. 2007, ApJ, 656, 437
3 Gregory, P. C. 2002, ApJ, 575, 427
4 Ackermann, M., Ajello, M., Ballet, J., et al. 2013, ApJ, 773, L35
5 Hadasch, D., Torres, D. F.,et al. 2012, ApJ, 749, 54
6 Jaron & Massi, 2014, A&A in press
7 Massi, M. & Jaron, F. 2013, A&A, 554, A105
8 Paredes, J. M.; Estalella, R. & Rius, A., 1990, A&A, 232, 377-380
9 Gregory, P. C., 1999, ApJ, 520, 376-390
10 Massi, M. & Torricelli-Ciamponi, G., 2014, A&A, 564, A23

Acknowledgements. Wavelet software was provided by C. Torrence and G. Compo, and is available at URL: http://atoc.colorado.edu/research/wavelets/.
The Green Bank Interferometer was operated by the National Radio Astronomy Observatory for the U.S. Naval Observatory and the Naval Research laboratory during the timeperiod of these observations.
This work has made use of public *Fermi* LAT data obtained from the High Energy Astrophysics Science Archive Research Center (HEASARC), provided by NASA Goddard Space Flight Center.